

## ON VARIATIONS OF THE BRIGHTNESS OF TYPE IA SUPERNOVAE WITH THE AGE OF THE HOST STELLAR POPULATION

BRENDAN K. KRUEGER<sup>1</sup>, AARON P. JACKSON<sup>1</sup>, DEAN M. TOWNSLEY<sup>2</sup>, ALAN C. CALDER<sup>1,3</sup>, EDWARD F. BROWN<sup>4</sup>, F. X. TIMMES<sup>5</sup>

*Accepted to the Astrophysical Journal Letters*

### ABSTRACT

Recent observational studies of type Ia supernovae (SNeIa) suggest correlations between the peak brightness of an event and the age of the progenitor stellar population. This trend likely follows from properties of the progenitor white dwarf (WD), such as central density, that follow from properties of the host stellar population. We present a statistically well-controlled, systematic study utilizing a suite of multi-dimensional SNeIa simulations investigating the influence of central density of the progenitor WD on the production of Fe-group material, particularly radioactive <sup>56</sup>Ni, which powers the light curve. We find that on average, as the progenitor's central density increases, production of Fe-group material does not change but production of <sup>56</sup>Ni decreases. We attribute this result to a higher rate of neutronization at higher density. The central density of the progenitor is determined by the mass of the WD and the cooling time prior to the onset of mass transfer from the companion, as well as the subsequent accretion heating and neutrino losses. The dependence of this density on cooling time, combined with the result of our central density study, offers an explanation for the observed age-luminosity correlation: a longer cooling time raises the central density at ignition thereby producing less <sup>56</sup>Ni and thus a dimmer event. While our ensemble of results demonstrates a significant trend, we find considerable variation between realizations, indicating the necessity for averaging over an ensemble of simulations to demonstrate a statistically significant result.

*Subject headings:* hydrodynamics — nuclear reactions, nucleosynthesis, abundances — supernovae: general — white dwarfs

### 1. INTRODUCTION

Observations targeting the environment of type Ia supernovae (SNeIa) have exposed open questions concerning the dependence of both their rates and average brightness on environment. Mannucci et al. (2006) show that the dependence of the SNIa rate on delay time (elapsed time between star formation and the supernova event) is best fit by a bimodal delay time distribution (DTD) with a prompt component less than 1 Gyr after star formation and a tardy component several Gyr later. Although the clarity of this effect is clouded by galaxy sampling (Filippenko 2009), the basic result is borne out even within galaxies (Raskin et al. 2009). Gallagher et al. (2008) measure a correlation between the brightness of a SNIa and its delay time, which they state is consistent with either a bimodal or a continuous DTD. Other recent studies by Howell et al. (2009), Neill et al. (2009), and Brandt et al. (2010) also find a correlation between the delay time and brightness of a SNIa.

Phillips (1993) identified a linear relationship between the maximum B-band magnitude of a light curve and its rate of decline. This “brighter equals broader” re-

lationship has been extended to additional bands with templates from nearby events, allowing SNeIa to be calibrated as an extension of the astronomical distance ladder (see Jha et al. 2007, for a description of one method). The brightness of a SNIa is determined principally by the radioactive decay of <sup>56</sup>Ni synthesized during the explosion (Truran et al. 1967; Colgate & McKee 1969; Arnett 1982; Pinto & Eastman 2000).

A widely-accepted proposal to explain many, if not most, events is the thermonuclear disruption of a white dwarf (WD) in a mass-transferring binary system (for reviews from various perspectives see: Branch et al. 1995; Filippenko 1997; Hillebrandt & Niemeyer 2000; Livio 2000; Röpke 2006). In this paradigm, a longer delay time suggests the possibility of a longer elapsed time between the formation of the WD and the onset of accretion. During this period, denoted here as the WD cooling time ( $t_{\text{cool}}$ ), the WD is isolated from any significant heat input and decreases in temperature. A longer  $t_{\text{cool}}$  results in a higher central density when the core reaches the ignition temperature (Lesaffre et al. 2006), due to the lower entropy at the onset of accretion. Thus, a correlation between central density and the peak brightness of an event suggests a correlation between delay time and the brightness of an event. While previous work indicated a correlation between central density and peak brightness, none has averaged over a statistically significant ensemble of realizations (Brachwitz et al. 2000; Röpke et al. 2006; Höflich et al. 2010). Therefore, we investigate, for the first time, a statistically significant correlation between progenitor central density and average peak brightness of SNeIa.

<sup>1</sup> Department of Physics & Astronomy, The State University of New York - Stony Brook, Stony Brook, NY

<sup>2</sup> Department of Physics and Astronomy, The University of Alabama, Tuscaloosa, AL

<sup>3</sup> New York Center for Computational Sciences, The State University of New York - Stony Brook, Stony Brook, NY

<sup>4</sup> Department of Physics and Astronomy, Michigan State University, East Lansing, MI

<sup>5</sup> School of Earth and Space Exploration, Arizona State University, Tempe, AZ, USA

The surrounding stellar population, the metallicity and mass of the progenitor, the thermodynamic state of the progenitor, the cooling and accretion history of the progenitor, and other parameters are known to affect the light curves of SNeIa; the role, and even primacy, of these various parameters is the subject of ongoing study (e.g., Röpke et al. 2006; Höflich et al. 2010; Jackson et al. 2010). Additionally, many of these effects may be interconnected in complex ways (Lesaffre et al. 2006). In this study, we isolate the direct effect of varying the progenitor central density on the production of  $^{56}\text{Ni}$ . To first order, this yield controls the brightness of an event; second-order effects on the light curve are left for future study.

## 2. METHOD

Once a WD forms in a binary, it is initially isolated and slowly cools in a single-degenerate scenario. Eventually, mass-transfer begins to carry light elements from the envelope of the companion to the surface of the WD. If the accretion rate exceeds a threshold, the infalling material experiences steady burning (Nomoto et al. 2007), and eventually the WD gains enough mass to compress and heat the core. Once the temperature rises enough to initiate carbon reactions, the core begins to convect (or “simmer”). Our progenitor models parameterize the WD at the end of this simmering phase, just prior to the birth of the flame that eventually will disrupt the entire WD in a SNIa.

We constructed a series of five parameterized, hydrostatic progenitor models that account for simmering in which we vary the central density ( $\rho_c$ ). The outer regions are isothermal, although some temperature structure is expected (Kuhlen et al. 2006), and the cores are isentropic due to convection and have a lower C/O ratio (Straniero et al. 2003; Piro & Bildsten 2008; Chamulak et al. 2008; Piro & Chang 2008). (Jackson et al. 2010) explored these effects and we chose the core composition as 40%  $^{12}\text{C}$ , 57%  $^{16}\text{O}$ , and 3%  $^{22}\text{Ne}$  and the outer layer as 50%  $^{12}\text{C}$ , 48%  $^{16}\text{O}$ , and 2%  $^{22}\text{Ne}$ . For our  $\rho_c$  we chose  $1 - 5 \times 10^9 \text{ g/cm}^3$  in steps of  $10^9 \text{ g/cm}^3$ . The central temperature must be in the range of carbon ignition, which is approximately  $7 - 8 \times 10^8 \text{ K}$  (e.g., Kuhlen et al. 2006); we selected  $7 \times 10^8 \text{ K}$ . Based on prior research, we chose other model parameters to produce expected amounts of Fe-group elements in the explosion (Townesley et al. 2009; Jackson et al. 2010). The values were kept constant in all simulations in order to isolate the central density effects.

With these five progenitor models, we utilize the statistical framework presented in Townesley et al. (2009) for a controlled study of the effect of varying the central density. For each progenitor, we created thirty realizations seeded by a random number used to generate a unique set of spherical harmonics with power in modes  $12 \leq \ell \leq 16$ . The spectra are used as initial perturbations to the spherical flame surface around the center of the progenitor star. Each progenitor uses the same seed values, resulting in the same thirty perturbations. This choice allows us to check for systematic biases in the realizations across different progenitors.

We performed a suite of 150 two-dimensional, axisymmetric simulations of the deflagration-to-detonation

transition (DDT) model of SNeIa with a customized version of FLASH, a compressible, Eulerian, adaptive-mesh, hydrodynamics code. The modifications to this code are (1) the burning model, (2) the flame speed computations, (3) the mesh refinement criteria, (4) the DDT criterion. Our simulation methods are described in detail in previous publications (Calder et al. 2007; Townesley et al. 2007, 2009) and continue to be improved (Jackson et al. 2010; Townesley et al. 2010). We should note that the DDT criterion is based on a characteristic density at which we ignite detonations, which we select to be  $10^{7.1} \text{ g/cm}^3$ . Following the procedures described in Calder et al. (2007) and Seitenzahl et al. (2009) for calculating the neutronization rate in material in nuclear statistical equilibrium (NSE), we utilize weak rates from Fuller et al. (1985), Oda et al. (1994), and Langanke & Martínez-Pinedo (2001), with newer rates superseding earlier ones. The reaction networks for calculating the energetics and time scales of the deflagration and detonation phases included the same 200 nuclides, and the NSE calculation of tables included 443 nuclides. The supernova simulations use a three-stage burning model in which the timescale to burn to NSE is calibrated to reproduce the correct yield of Fe-group elements. The weak reaction rate is negligible at a density where Si-burning to  $^{56}\text{Ni}$  is incomplete; therefore, we estimate the  $^{56}\text{Ni}$  yield from the total NSE yield and its associated electron fraction. We performed nuclear postprocessing of Lagrangian tracer particles using a network of 200 nuclides on a subset of simulations. Comparison demonstrates that our burning model matches the energetics and final composition of important nuclei such as  $^{56}\text{Ni}$  (Townesley et al. 2010) (see also studies by Travaglio et al. 2004; Seitenzahl et al. 2010). We utilize the adaptive-mesh capability, with a highest resolution of 4 km, which demonstrates a converged result (Townesley et al. 2009).

## 3. RESULTS AND DISCUSSION

The  $^{56}\text{Ni}$  yield is determined partly by neutronization occurring during the thermonuclear burning. Neutronization pushes the nucleosynthetic yield away from balanced nuclei such as  $^{56}\text{Ni}$  to more neutron-rich, stable isotopes like  $^{58}\text{Ni}$ . Thus the amount of neutronization influences the brightness of an event and, all else being constant, more neutronization results in a dimmer event. The degree of neutronization depends on the density and temperature evolution of burned material. Generally, thermonuclear burning occurring at higher densities will neutronize faster. In an explosive event like a supernova, the longer material remains in NSE at high densities, the more neutronization occurs (Nomoto et al. 1984; Khokhlov 1991; Calder et al. 2007). Accordingly, for SNeIa, both the central density and the duration of the deflagration phase influence the brightness of an event.

Figure 1 presents the mass fraction of NSE material that is  $^{56}\text{Ni}$  as a function of deflagration duration, with points colored to indicate  $\rho_c$ . The duration of the deflagration phase is the time elapsed between the formation of a flame front and the ignition of the first detonation point. We consider this elapsed time because there is little contribution to neutronization after the first DDT. The mass of NSE material produced increases during the

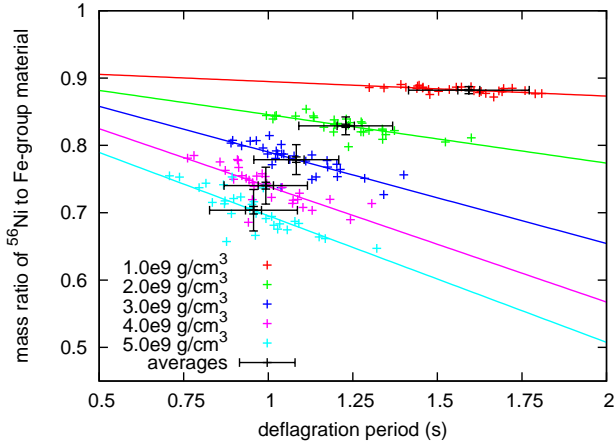


FIG. 1.— Plot of the  $^{56}\text{Ni}$ -to-NSE mass ratio vs. duration of deflagration. Small crosses are single simulations and are colored by  $\rho_c$ . Large black crosses show the average values for a given  $\rho_c$  with error bars showing the standard deviation and the standard error of the mean.

course of the SNIa and eventually plateaus; we find the point where the NSE yield changes by less than 0.01% over 0.01 s and use that mass as the final yield of the SNIa. The results have considerable scatter but show two trends. First, at a given  $\rho_c$ , simulations with longer deflagration periods tend to have a greater degree of neutronization. Next, simulations from progenitors with higher central densities tend to have a greater degree of neutronization despite having shorter deflagration periods. This result shows that the increased rate of neutronization at higher densities, which can be seen by the steeper slopes of the higher density trend lines, more than compensates for the decrease in time for neutronization to occur. Accordingly, our results qualitatively agree with previous work (e.g., Iwamoto et al. 1999; Brachwitz et al. 2000; Höflich et al. 2010). We also note that the yield of NSE material is, within the error of the slope, independent of  $\rho_c$ . As seen in Woosley et al. (2007), if the NSE yield remains constant but the amount of  $^{56}\text{Ni}$  varies, then the results should lie along the Phillips relation.

The greater degree of neutronization seen in Figure 1 leads directly to lower  $^{56}\text{Ni}$  yields with increasing  $\rho_c$ . This result can be seen in Figure 2, which presents the  $^{56}\text{Ni}$  yield of each simulation plotted against  $\rho_c$  with color used to classify the simulations by realization. The scatter among different realizations at the same  $\rho_c$  is greater than the variation across the  $\rho_c$  range, indicating the need for analysis of an ensemble of realizations. This scatter can result in a single realization showing a trend unlike the statistical trend; for example, by considering only realization 2 and  $\rho_c$  of  $2 \times 10^9$  and  $3 \times 10^9$  g/cm $^3$  (Figure 2, green curve), we would conclude that increasing  $\rho_c$  causes an increase in  $^{56}\text{Ni}$  production, instead of a decrease as seen in the overall ensemble. The scatter follows from a strong dependence on the morphology of the flame surface during the early deflagration, which varies the duration of the deflagration and the production of  $^{56}\text{Ni}$ . Changing  $\rho_c$  can cause a local change in the plume dynamics that overrides the general trend. By fitting the averages we find the relation

$$M_{56\text{Ni}} = A\rho_c + B, \quad (1)$$

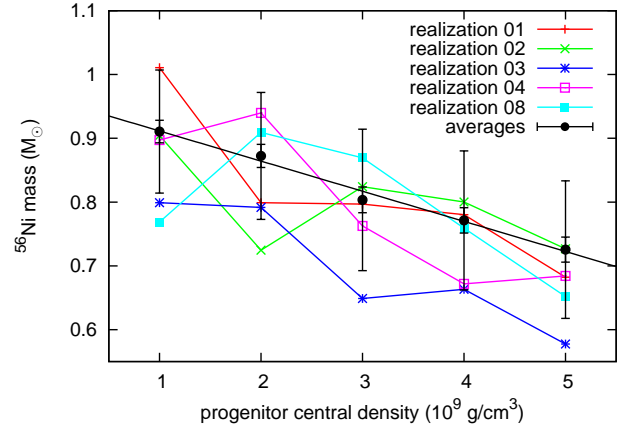


FIG. 2.— Plot of mass of  $^{56}\text{Ni}$  produced vs.  $\rho_c$  for five different realizations (colored curves), demonstrating the variety of trends seen for a single realization. These include non-monotonic trends, which could suggest an increase of  $^{56}\text{Ni}$  with increasing  $\rho_c$  instead of the decrease seen in the ensemble. In black are the average values for each density, along with the standard deviation, the standard error of the mean, and a regression fit to the average values.

where

$$A = -0.047 \pm 0.003 \frac{M_\odot}{10^9 \text{g/cm}^3}$$

$$B = 0.959 \pm 0.009 M_\odot.$$

We use data from Lesaffre et al. (2006) to correlate  $\rho_c$  to  $t_{\text{cool}}$ , one component of the delay time, specifically the results for a WD with a pre-accretion mass of  $1 M_\odot$ . Thus if we imagine a collection of stars forming with the same zero-age main-sequence mass but with different companions and binary separations, the delay time would be dominated by  $t_{\text{cool}}$ . There are large uncertainties in the relationship between  $\rho_c$  and  $t_{\text{cool}}$ ; accordingly, we neglect error derived from this large uncertainty in our analysis. We note that the work of Lesaffre et al. (2006) suggests that a WD with a central density of  $10^9$  g/cm $^3$  will not ignite; further accretion is necessary to reach ignition conditions. Therefore we cannot use Lesaffre et al. (2006) to compute a  $t_{\text{cool}}$  for our lowest- $\rho_c$  simulations, and so we omit such simulations.

We convert our  $^{56}\text{Ni}$  mass to stretch (s) (Howell et al. 2009), the magnitude difference in the B band between maximum light and 15 days after maximum light ( $\Delta m_{15}(B)$ ) (Goldhaber et al. 2001), and absolute magnitude in the V band at maximum light ( $M_V$ ) (Phillips et al. 1999) in order to compare with observational findings, shown in Figure 3. A detailed comparison of our models to these observables requires radiative transport calculations of synthetic spectra and light curves, but our results drawn from the  $^{56}\text{Ni}$  mass are sufficient for the basic properties we consider here. Woosley et al. (2007) showed that the brightness of an event depends on the mass of  $^{56}\text{Ni}$  when it is distributed through a large fraction of the star as in our simulations. Additionally, Stritzinger et al. (2006) showed that late-time nebular spectroscopy finds  $^{56}\text{Ni}$  yields consistent with those found from peak luminosity using the inverse of the relations we use.

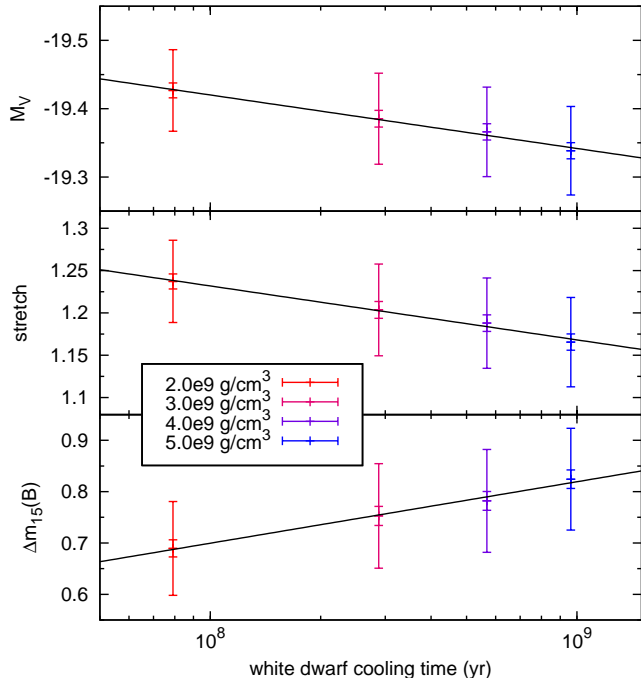


FIG. 3.— Plot of brightness vs.  $t_{\text{cool}}$  in terms of  $M_V$  (upper panel),  $s$  (central panel), and  $\Delta m_{15}(B)$  (lower panel). Plotted are the average values for each  $\rho_c$  along with the standard deviation, the standard error of the mean, and a regression fit to the average values.

TABLE 1  
BEST-FIT PARAMETERS FOR BRIGHTNESS-AGE RELATIONS.

$q$	$\alpha_q$	$\beta_q$
$M_V$	$0.078 \pm 0.006$	$-20.05 \pm 0.05$
$s$	$-0.064 \pm 0.005$	$1.74 \pm 0.04$
$\Delta m_{15}(B)$	$0.120 \pm 0.009$	$-0.26 \pm 0.08$

We find that the best-fit relations follow the form

$$q = \alpha_q \log_{10} \left( \frac{t_{\text{cool}}}{\text{yr}} \right) + \beta_q \quad (2)$$

where  $q$  is one of  $\Delta m_{15}(B)$ ,  $s$ , or  $M_V$ . The values for  $\alpha_q$  and  $\beta_q$  are shown in Table 1.

To highlight the comparison with observations, in Figure 4 we plot an expansion of the center panel from Figure 3 with the binned results from Figure 5 of Neill et al. (2009). While an absolute comparison is not possible, the similarity of the overall trend indicates that variation of  $\rho_c$  is an important contribution to the observed dependence. Our choice of initial conditions and DDT density results in an effective calibration that yields higher than expected  $^{56}\text{Ni}$  masses. Accordingly, our results are systematically too bright, giving abnormally high values of stretch. Future studies will correct for this effect. A more subtle point comes in the usage of “age”: Neill et al. (2009) measures the luminosity-weighted stellar age, while for the theory we have simply used  $t_{\text{cool}}$  directly, which for late times is the dominant portion of the time elapsed since star formation. Such offsets, either vertical or horizontal, are less important than the overall trend and the range that can be attributed to variation of  $\rho_c$ . For comparison, the black line in Fig-

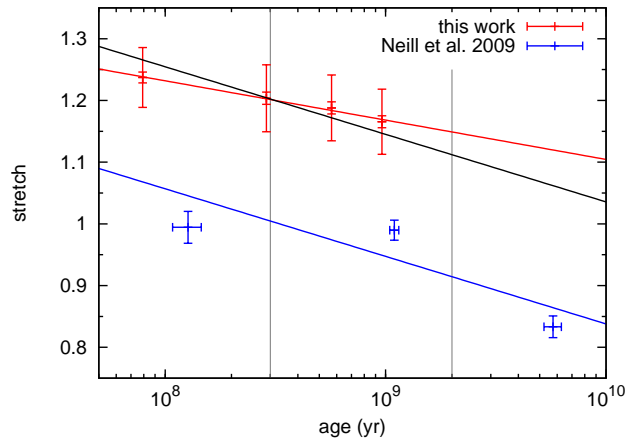


FIG. 4.— Plot of stretch vs. age. In red are the points from this study, based on variations in  $\rho_c$ , along with the standard deviation, the standard error of the mean, and a best-fit trend line following the form of Equation (2). In blue are the binned and averaged points from Figure 5 of Neill et al. (2009), along with a best-fit trend line following the form of Equation (2). The vertical grey lines mark the cuts between bins in the Neill et al. (2009) analysis. The trend line for the Neill et al. (2009) data is shifted upward for comparison to our results (black line). The overall offset to larger stretch in the simulations is due to the choice of DDT density. The approximate agreement of the overall trend indicates that the variation of  $\rho_c$  is an important contributor to the observed trend, but that other factors are also important.

ure 4 shifts the best-fit line from the data of Neill et al. (2009) up to align it with our results. The trend due to  $\rho_c$  is weaker than in observations, suggesting that  $\rho_c$  contributes to the observed trend but that other effects also play a part.

#### 4. CONCLUSIONS AND FUTURE WORK

We simulated a suite of 150 SNIa models with a range of  $\rho_c$  to study the trends for a population of SNeIa. We find that on average progenitors with higher  $\rho_c$  produce less  $^{56}\text{Ni}$ . Höflich et al. (2010) argue that  $^{56}\text{Ni}$  in the central regions of the exploding WD does not contribute to the light curve at maximum, and therefore they do not see a significant trend with central density in the maximum V-band magnitude, but rather in late-time brightness. The pure-deflagration models of Röpke et al. (2006) exhibit a shallow increase of produced  $^{56}\text{Ni}$  as central density increases, in contradiction of our findings. Iwamoto et al. (1999) find that the trend with central density depends on the DDT transition density; extrapolating from their results, our value of  $\rho_{\text{DDT}}$  should yield an increasing  $^{56}\text{Ni}$  yield as central density increases. We find that small perturbations of the initial flame surface not only influence the final  $^{56}\text{Ni}$  yield, but also its dependence on central density through variations in the duration of the deflagration phase caused by differences in plume development. The variation that follows from perturbations on the initial conditions is a critical aspect of multi-dimensional modeling. Only after many realizations with different perturbations of the initial flame surface are simulated does a statistically significant trend with central density emerge. This result, illustrated by Figure 2, demonstrates the need for an ensemble of simulations to explore systematic effects in SNeIa.

By relating  $\rho_c$  to  $t_{\text{cool}}$  and  $^{56}\text{Ni}$  to  $\Delta m_{15}(B)$ , our results support the observational finding that SNeIa from older

stellar populations are systematically dimmer. While a degeneracy between age and metallicity in the integrated light of stellar populations exists, the observed dependence of mean brightness of SNeIa on mean stellar age is apparently the stronger effect (Gallagher et al. 2008; Howell et al. 2009). Accordingly, our choice to neglect metallicity effects and consider only the effect of central density on  $^{56}\text{Ni}$  yield allows us to offer a theoretical explanation for this observed trend. If we additionally consider the effect of metallicity, we may see a slightly stronger trend of decreasing brightness with increasing age as has been previously suggested (Timmes et al. 2003). Other effects besides progenitor central density and metallicity, such as progenitor main sequence mass, may also contribute to this trend.

The insensitivity of the overall Fe-group yield to central density, and therefore delay time, along with the dependence of the  $^{56}\text{Ni}$  yield on central density, implies that SNeIa of similar brightnesses (and therefore similar  $^{56}\text{Ni}$  yield) from progenitors of different ages will not have the same total Fe-group yield. Those from older populations will, on average, have larger masses of stable species. This may argue for a slight non-uniformity in the Phillips relation based on environment (Woosley et al. 2007; Höflich et al. 2010). The resulting closely-related family of brightness-decline time relations also provides a physical motivation for intrinsic scatter in the Phillips relation as a result of combining populations with different mean stellar ages. In this picture the primary parameter is the degree of expansion at DDT, determined by the morphology of the early flame (and the DDT den-

sity, which we hold constant), and the age acts a weaker secondary parameter. In any case, the possibility of such an effect motivates further exploration of the impact of central density on the light curve itself.

This work was supported by the Department of Energy through grants DE-FG02-07ER41516, DE-FG02-08ER41570, and DE-FG02-08ER41565, and by NASA through grant NNX09AD19G. ACC also acknowledges support from the Department of Energy under grant DE-FG02-87ER40317. DMT received support from the Bart J. Bok fellowship at the University of Arizona for part of this work. The authors gratefully acknowledge the generous assistance of Pierre Lesaffre, as well as fruitful discussions with Mike Zingale, and the use of NSE and weak reaction tables developed by Ivo Seitenzahl. The authors also acknowledge the hospitality of the KITP, which is supported by NSF grant PHY05-51164, during the programs “Accretion and Explosion: the Astrophysics of Degenerate Stars” and “Stellar Death and Supernovae.” The software used in this work was in part developed by the DOE-supported ASC/Alliances Center for Astrophysical Thermonuclear Flashes at the University of Chicago. This research utilized resources at the New York Center for Computational Sciences at Stony Brook University/Brookhaven National Laboratory which is supported by the U.S. Department of Energy under Contract No. DE-AC02-98CH10886 and by the State of New York.

## REFERENCES

- Arnett, W. D. 1982, *ApJ*, 253, 785
- Brachwitz, F., Dean, D. J., Hix, W. R., Iwamoto, K., Langanke, K., Martínez-Pinedo, G., Nomoto, K., Strayer, M. R., Thielemann, F., & Umeda, H. 2000, *ApJ*, 536, 934
- Branch, D., Livio, M., Yungelson, L. R., Boffi, F. R., & Baron, E. 1995, *PASP*, 107, 1019
- Brandt, T. D., Tojeiro, R., Aubourg, É., Heavens, A., Jimenez, R., & Strauss, M. A. 2010, *ArXiv e-prints*
- Calder, A. C., Townsley, D. M., Seitenzahl, I. R., Peng, F., Messer, O. E. B., Vladimirova, N., Brown, E. F., Truran, J. W., & Lamb, D. Q. 2007, *ApJ*, 656, 313
- Chamulak, D. A., Brown, E. F., Timmes, F. X., & Dupczak, K. 2008, *ApJ*, 677, 160
- Colgate, S. A. & McKee, C. 1969, *ApJ*, 157, 623
- Filippenko, A. V. 1997, *ARA&A*, 35, 309
- Filippenko, A. V. 2009, in *Stellar Death and Supernovae*
- Fuller, G. M., Fowler, W. A., & Newman, M. J. 1985, *ApJ*, 293, 1
- Gallagher, J. S., Garnavich, P. M., Caldwell, N., Kirshner, R. P., Jha, S. W., Li, W., Ganeshalingam, M., & Filippenko, A. V. 2008, *ApJ*, 685, 752
- Goldhaber, G., Groom, D. E., Kim, A., Aldering, G., Astier, P., Conley, A., Deustua, S. E., Ellis, R., Fabbro, S., Fruchter, A. S., Goobar, A., Hook, I., Irwin, M., Kim, M., Knop, R. A., Lidman, C., McMahon, R., Nugent, P. E., Pain, R., Panagia, N., Pennypacker, C. R., Perlmutter, S., Ruiz-Lapuente, P., Schaefer, B., Walton, N. A., & York, T. 2001, *ApJ*, 558, 359
- Hillebrandt, W. & Niemeyer, J. C. 2000, *ARA&A*, 38, 191
- Höflich, P., Krisciunas, K., Khokhlov, A. M., Baron, E., Folatelli, G., Hamuy, M., Phillips, M. M., Suntzeff, N., Wang, L., & NSF07-SNIa Collaboration. 2010, *ApJ*, 710, 444
- Howell, D. A., Sullivan, M., Brown, E. F., Conley, A., LeBorgne, D., Hsiao, E. Y., Astier, P., Balam, D., Balland, C., Basa, S., Carlberg, R. G., Fouchez, D., Guy, J., Hardin, D., Hook, I. M., Pain, R., Perrett, K., Pritchett, C. J., Regnault, N., Baumont, S., LeDu, J., Lidman, C., Perlmutter, S., Suzuki, N., Walker, E. S., & Wheeler, J. C. 2009, *ApJ*, 691, 661
- Iwamoto, K., Brachwitz, F., Nomoto, K., Kishimoto, N., Umeda, H., Hix, W. R., & Thielemann, F. 1999, *ApJS*, 125, 439
- Jackson, A. P., Calder, A. C., Townsley, D. M., Chamulak, D. A., Brown, E. F., & Timmes, F. X. 2010, *ApJ*, submitted
- Jha, S., Riess, A. G., & Kirshner, R. P. 2007, *ApJ*, 659, 122
- Khokhlov, A. M. 1991, *A&A*, 245, L25
- Kuhlen, M., Woosley, S. E., & Glatzmaier, G. A. 2006, *ApJ*, 640, 407
- Langanke, K. & Martínez-Pinedo, G. 2001, *At. Data Nucl. Data Tables*, 79, 1
- Lesaffre, P., Han, Z., Tout, C. A., Podsiadlowski, P., & Martin, R. G. 2006, *MNRAS*, 368, 187
- Livio, M. 2000, in *Type Ia Supernovae, Theory and Cosmology*, ed. J. C. Niemeyer & J. W. Truran, 33–
- Mannucci, F., Della Valle, M., & Panagia, N. 2006, *MNRAS*, 370, 773
- Neill, J. D., Sullivan, M., Howell, D. A., Conley, A., Seibert, M., Martin, D. C., Barlow, T. A., Foster, K., Friedman, P. G., Morrissey, P., Neff, S. G., Schiminovich, D., Wyder, T. K., Bianchi, L., Donas, J., Heckman, T. M., Lee, Y., Madore, B. F., Milliard, B., Rich, R. M., & Szalay, A. S. 2009, *ApJ*, 707, 1449
- Nomoto, K., Saio, H., Kato, M., & Hachisu, I. 2007, *ApJ*, 663, 1269
- Nomoto, K., Thielemann, F.-K., & Yokoi, K. 1984, *ApJ*, 286, 644
- Oda, T., Hino, M., Muto, K., Takahara, M., & Sato, K. 1994, *Atomic Data and Nuclear Data Tables*, 56, 231
- Phillips, M. M. 1993, *ApJ*, 413, L105
- Phillips, M. M., Lira, P., Suntzeff, N. B., Schommer, R. A., Hamuy, M., & Maza, J. 1999, *AJ*, 118, 1766
- Pinto, P. A. & Eastman, R. G. 2000, *ApJ*, 530, 744
- Piro, A. L. & Bildsten, L. 2008, *ApJ*, 673, 1009
- Piro, A. L. & Chang, P. 2008, *ApJ*, 678, 1158
- Raskin, C., Scannapieco, E., Rhoads, J., & Della Valle, M. 2009, *ApJ*, 707, 74
- Röpke, F. K. 2006, in *Reviews in Modern Astronomy*, Vol. 19, *Reviews in Modern Astronomy*, ed. S. Roeser, 127–

- Röpke, F. K., Gieseler, M., Reinecke, M., Travaglio, C., & Hillebrandt, W. 2006, *A&A*, 453, 203
- Seitenzahl, I. R., Röpke, F., Fink, M., & Pakmor, R. 2010, *ArXiv e-prints*
- Seitenzahl, I. R., Townsley, D. M., Peng, F., & Truran, J. W. 2009, *Atomic Data and Nuclear Data Tables*, 95, 96
- Straniero, O., Domínguez, I., Imbriani, G., & Piersanti, L. 2003, *ApJ*, 583, 878
- Stritzinger, M., Mazzali, P. A., Sollerman, J., & Benetti, S. 2006, *A&A*, 460, 793
- Timmes, F. X., Brown, E. F., & Truran, J. W. 2003, *ApJ*, 590, L83
- Townsley, D. M., Calder, A. C., Asida, S. M., Seitenzahl, I. R., Peng, F., Vladimirova, N., Lamb, D. Q., & Truran, J. W. 2007, *ApJ*, 668, 1118
- Townsley, D. M., Jackson, A. P., Calder, A. C., Chamulak, D. A., Brown, E. F., & Timmes, F. X. 2009, *ApJ*, 701, 1582
- Townsley, D. M., Timmes, F. X., Jackson, A. P., Calder, A. C., & Brown, E. F. 2010, in prep
- Travaglio, C., Hillebrandt, W., Reinecke, M., & Thielemann, F. 2004, *A&A*, 425, 1029
- Truran, J. W., Arnett, W. D., & Cameron, A. G. W. 1967, *Canadian Journal of Physics*, 45, 2315
- Woosley, S. E., Kasen, D., Blinnikov, S., & Sorokina, E. 2007, *ApJ*, 662, 487